

MEAL: A Benchmark for Continual Multi-Agent Reinforcement Learning

Tristan Tomilin¹ Luka van den Boogaard¹ Samuel Garcin²
 Bram Grooten¹ Meng Fang^{3,1} Mykola Pechenizkiy¹

¹Eindhoven University of Technology ²University of Edinburgh ³University of Liverpool

{t.tomilin,l.v.d.boogaard,b.grooten,m.pechenizkiy}@tue.nl
 s.garcin@ed.ac.uk meng.fang@liverpool.ac.uk

Abstract

Benchmarks play a crucial role in the development and analysis of reinforcement learning (RL) algorithms, with environment availability strongly impacting research. One particularly underexplored intersection is continual learning (CL) in cooperative multi-agent settings. To remedy this, we introduce **MEAL** (Multi-agent Environments for Adaptive Learning), the first benchmark tailored for continual multi-agent reinforcement learning (CMARL). Existing CL benchmarks run environments on the CPU, leading to computational bottlenecks and limiting the length of task sequences. MEAL leverages JAX for GPU acceleration, enabling continual learning across sequences of 100 tasks on a standard desktop PC in a few hours. We show that naïvely combining popular CL and MARL methods yields strong performance on simple environments, but fails to scale to more complex settings requiring sustained coordination and adaptation. Our ablation study identifies architectural and algorithmic features critical for CMARL on MEAL.

1 Introduction

Continual RL has recently attracted growing interest [13, 7, 8, 11], but remains largely unexplored in multi-agent settings [34, 35]. Combining the two introduces unique challenges. In cooperative environments, agents must establish implicit conventions or roles for effective coordination [28]. As tasks or dynamics shift, these conventions can break down, making continual MARL significantly harder than its single-agent counterpart. Forgetting past partners or roles can cause the entire team to fail, amplifying the impact of catastrophic forgetting through inter-agent dependencies. Unlike traditional MARL, CMARL involves non-stationarity not only due to the presence of other learning agents, but also from a shifting task distribution [35]. This dual pressure demands agents that can generalize, adapt, and transfer knowledge more robustly than in standard single-agent continual or static multi-agent settings. This setting is relevant for applications where agents must adapt to evolving environments without forgetting prior coordination strategies. For instance, autonomous vehicles must navigate unseen roads, adapt to new traffic regulations, and interact with unfamiliar human drivers, while occasionally coordinating with other AVs. Similarly, warehouse robots deployed in a new facility must quickly adapt to different layouts and workflows, while preserving established collaborative behaviors.

To analyze how current methods handle the interplay between CL and MARL, and to drive progress in this domain, we introduce **MEAL**, the first benchmark for CMARL. To the best of our knowledge, MEAL¹ is also the first continual RL library to leverage JAX for end-to-end GPU acceleration. Traditional CPU-based benchmarks are limited to short sequences (5–15 tasks) due to low environment

¹The code and environments are accessible on GitHub.

Table 1: Comparison of existing Reinforcement Learning benchmarks with MEAL.

Benchmark	No. Tasks	Difficulty Levels	GPU-accelerated	Action Space	Multi-Agent	Continual Learning
CORA [23]	31	✗	✓	Mixed	✗	✓
MPE [21]	7	✗	✗	Continuous	✓	✗
SMAC [26]	14	✓	✗	Discrete	✓	✗
Continual World [31]	10	✗	✗	Continuous	✗	✓
Melting Pot [2]	49	✗	✗	Discrete	✓	✗
Google Football [18]	14	✓	✓	Discrete	✓	✗
JaxMARL [25]	33	✗	✓	Mixed	✓	✗
COOM [30]	8	✓	✗	Discrete	✗	✓
MEAL	∞	✓	✓	Discrete	✓	✓

throughput and task diversity [27, 23, 30], making them ill-suited for the computational demands of CL across long task sequences. MEAL’s end-to-end JAX pipeline removes this barrier, enabling training on up to 100 tasks within a few hours on a single desktop GPU. This unlocks new research directions for scalable, cooperative continual learning in resource-constrained settings.

MEAL is built on Overcooked [6], a widely used cooperative MARL environment [15, 32, 28] that provides a strong foundation for benchmarking. Prior work has shown that agents tend to exploit spurious correlations in fixed layouts, resulting in poor generalization even under minor modifications [17]. This makes Overcooked particularly well-suited for continual learning: even small layout variations can present a significant challenge. To succeed across a sequence of such tasks, agents must avoid overfitting to layout-specific behaviors and instead learn coordination strategies that are robust and transferable.

The **contributions** of our work are three-fold. (1) We introduce MEAL, the first CMARL benchmark, consisting of handcrafted and procedurally generated Overcooked environments spanning three difficulty levels. (2) We leverage JAX to build the first end-to-end GPU-accelerated task sequences for continual RL, enabling efficient training on low-budget setups. (3) We implement five popular CL methods in JAX and evaluate them in various MEALs, revealing key shortcomings in retaining cooperative behaviors and adapting to shifting roles across tasks.

2 Related Work

Continual Reinforcement Learning (CRL) Continual reinforcement learning studies how agents can learn sequentially from a stream of tasks without forgetting previous knowledge. A wide range of methods have been proposed, including regularization-based approaches such as EWC [16], SI [36], and MAS [3]; architectural strategies such as PackNet [20]; and replay-based methods like RePR [4]. More recent works focus on scalability [13], memory efficiency [8], and stability during training [7]. However, these methods are almost exclusively developed for single-agent settings, and their behavior under multi-agent coordination remains largely unexplored.

Multi-Agent Reinforcement Learning (MARL) In MARL, multiple agents learn to act in a shared environment, often with partial observability and either cooperative or competitive goals [14, 22]. A major focus has been on cooperative settings, where agents share a reward function and must learn to coordinate [19, 12]. Popular algorithms include IPPO [9], VDN [29], QMIX [24], and MAPPO [33]. Many benchmarks assume a static environment and fixed task, making them unsuitable for studying continual learning or transfer across environments.

Benchmarks Standard CRL benchmarks include Continual World [31], COOM [30], and CORA [23]. While effective in single-agent settings, they either lack multi-agent capabilities or suffer from slow CPU-bound environments. For MARL, environments like SMAC [26], MPE [21], and Melting Pot [2] are widely used, but are not designed for continual evaluation. Overcooked [6] has emerged as a useful domain for studying coordination, with recent implementations in JAX [25]. Our benchmark builds on Overcooked and introduces procedural variation to create long task sequences for continual MARL.

Overcooked The Overcooked environment [6] is a cooperative multi-agent benchmark inspired by the popular video game of the same name. Agents control chefs in a grid-based kitchen, coordinating to prepare and deliver dishes through sequences of interactions with environment objects such as pots, ingredient dispensers, plate stations, and delivery counters. The environment is designed to require both motion and strategy coordination, making it a standard testbed for evaluating collaborative behaviors. Compared to the large state spaces and high agent counts in benchmarks like Melting Pot [2] and SMAC [26], Overcooked operates on small grid-based environments with only two agents. However, its complexity arises not from scale but from credit assignment challenges due to shared rewards, and the need for precise coordination, as agents must execute tightly coupled action sequences to complete tasks successfully [14]. However, its fully observable and symmetric setup reduces the need for explicit communication.

3 Preliminaries

Cooperative Multi-Agent MDP We formulate the setting as a fully observable cooperative multi-agent task, modeled as a Markov game defined by the tuple $\langle N, S, A^i_{i \in N}, P, R, \gamma \rangle$, where N is the number of agents, S is the state space, A^i is the action space of agent i with joint action space $A = A^1 \times \dots \times A^N$, $P : S \times A \times S \rightarrow [0, 1]$ is the transition function, $R : S \times A \times S \rightarrow \mathbb{R}$ is a shared reward function, and $\gamma \in [0, 1)$ is the discount factor. In the fully observable setting, each agent receives the full state $s \in S$ at every time step.

Continual MARL We consider a continual MARL setting in which a shared policy $\pi_\theta = \pi_{\theta^i}^i_{i \in N}$ is learned over a sequence of tasks $\mathcal{T} = \mathcal{M}_1, \dots, \mathcal{M}_T$, where each $\mathcal{M}_t = \langle N, S_t, A^i_{i \in N}, P_t, R_t, \gamma \rangle$ is a fully observable cooperative Markov game with consistent action and observation spaces. At training phase t , agents interact exclusively with \mathcal{M}_t for a fixed number of iterations Δ , collecting trajectories $\tau_{t,1}, \dots, \tau_{t,\Delta}$ to update their policy. Past tasks and data are inaccessible, and no joint training or replay is allowed. The focus of this work is on the task-incremental setting, where the task identity is known during training but hidden at evaluation. The objective is to maximize cumulative performance across all tasks and mitigate forgetting.

4 MEAL

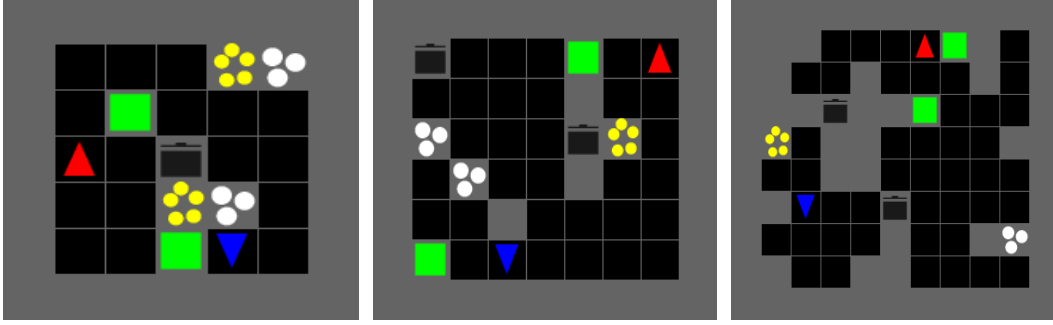
We introduce MEAL, the first benchmark for CMARL, built on the JaxMARL [25] version of Overcooked. JAX [5] provides just-in-time compilation, automatic differentiation, and vectorization through XLA, enabling high-performance and accelerator-agnostic computation. We incorporate the original five layouts from Overcooked-AI [6] and design 20 additional handcrafted environments.

4.1 Environment Dynamics

Observations Each agent receives a fully observable grid-based observation of shape $(H, W, 26)$, where H and W are the height and width of the environment, and the 26 channels encode entity types (e.g., walls, agents, onions, plates, pots, delivery stations) and object states (e.g., cooking progress, held item). To ensure compatibility across environments in a continual learning setting, we fix H_{\max} and W_{\max} to the largest layout size and pad smaller layouts with walls. Observations are then standardized to the shape $(H_{\max}, W_{\max}, 26)$.

Action Space At each timestep, both agents select one of six discrete actions from a shared action space $\mathcal{A} = \{\text{up}, \text{down}, \text{left}, \text{right}, \text{stay}, \text{interact}\}$. Movement actions translate the agent forward if the target tile is free (i.e., not a wall or occupied), while `stay` maintains the current position. The `interact` action is context-dependent and allows agents to pick up or place items, add ingredients to pots, serve completed dishes, or deliver them at the goal location. Importantly, there is no built-in communication action; all coordination emerges from environment interactions.

Rewards Agents receive a shared team reward: $r_t = r_{\text{deliver}} + r_{\text{onion}} \cdot \mathbb{1}_{\{\text{onion_in_pot}\}} + r_{\text{plate}} \cdot \mathbb{1}_{\{\text{plate_pickup}\}} + r_{\text{soup}} \cdot \mathbb{1}_{\{\text{soup_pickup}\}}$, where $r_{\text{deliver}} = 20$ is the reward for delivering a cooked soup, and the remaining terms provide shaped rewards for intermediate progress. We include two reward settings: in the **sparse** setting, $r_{\text{onion}} = r_{\text{plate}} = r_{\text{soup}} = 0$; in the **dense** setting, $r_{\text{onion}} = r_{\text{plate}} = 3$, and $r_{\text{soup}} = 5$.



(a) **Level 1 (Easy):** $6 \leq \text{width/height} \leq 7$, obstacle density $\approx 15\%$. Layouts are compact, making exploration easy. Interactable items are close together, and travel distances are short. Agents can often complete the task independently with minimal coordination.

(b) **Level 2 (Medium):** $8 \leq \text{width/height} \leq 9$, obstacle density $\approx 25\%$. Exploration becomes harder as key items are more spread out. Layouts often introduce choke-points, requiring agents to coordinate movement and avoid congestion.

(c) **Level 3 (Hard):** $10 \leq \text{width/height} \leq 11$, obstacle density $\approx 35\%$. Layouts are more likely to split the map into disjoint regions, forcing agents to specialize. Solving the task requires deliberate cooperation and division of labor.

Figure 1: Representative Overcooked layouts generated at each difficulty level. Increasing grid size and obstacle density lead to longer travel distances, harder exploration, and greater coordination demands.

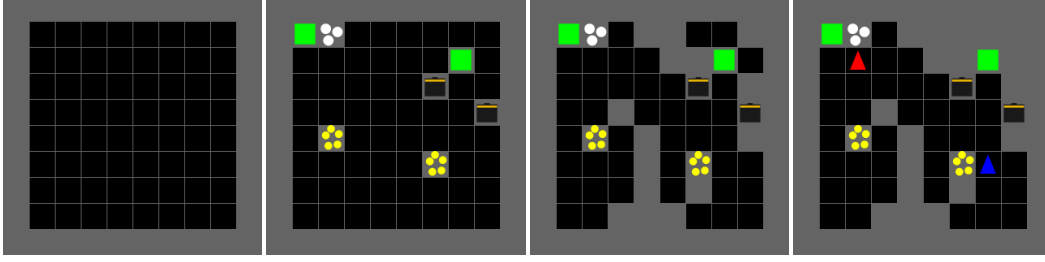
Score Function We measure performance as the total number of soups successfully delivered by the team during an episode. Since MEAL layouts vary in size, structure, and the number of interactive elements, the maximum number of soups that can be delivered in a fixed time horizon differs across tasks. To allow fair comparisons across sequences and environments, we normalize returns using a programmatically computed performance estimate. For each layout we estimate the fastest possible *single-agent* cook-deliver cycle, accounting for the shortest paths between onion piles, pots, plate piles, and delivery counters, the fixed cooking time, and pickup/drop interactions. Repeating this cycle over the episode length yields a soup total estimate. This ratio equals 1 when an agent matches the single-agent optimum and can exceed 1 if multiple agents collaborate more efficiently than our single-agent model assumes. A detailed description can be found in Appendix A.1.

4.2 MEAL Generator

Existing continual RL benchmarks only provide a fixed set of tasks [27, 23, 30]. To avoid over-fitting to a fixed set of environments, we procedurally generate new Overcooked kitchens on the fly. The generator draws a random width and height from the specified range, places an outer wall, then sequentially injects the interactive tiles (goal, pot, onion pile, plate pile), extra internal walls to match the target obstacle density, and finally, the agents’ starting positions. Figure 2 depicts the pipeline, and the process is described more in-depth in Appendix A.2. Each candidate grid is accepted only if a built-in validator module confirms that both agents can complete at least one cook-deliver cycle. This yields a continuous space of solvable, variable-sized kitchens that we can learn continually. We bring further details about the validator in Appendix A.3. Our approach offers a virtually infinite supply of tasks and evaluates true lifelong learning under continual exposure to unseen configurations. To ensure reproducibility and a fair comparison between methods, the generation process can be fully controlled via a user-specified random seed.

4.3 Layout Difficulty

We categorize environment difficulty based on procedurally generated layout characteristics. We vary the (1) grid width, (2) grid height, and (3) obstacle density. This approach produces diverse spatial configurations while maintaining consistent difficulty within each level. Figure 1 illustrates representative layouts for each difficulty tier. As grid size and the number of impassable tiles increase, agents must develop more sophisticated coordination strategies. Higher difficulty layouts feature longer paths between key items, tighter bottlenecks, and greater structural variability, all of which make exploration, retention, and adaptation more challenging. Appendix C.1 presents a performance



(a) Empty grid with outer walls (b) Interactive stations randomly placed (c) Grid filled with walls to match obstacle density (d) Agents added & unreachable tiles pruned

Figure 2: Procedural generation pipeline of a **hard** layout. Starting from an empty grid with outer walls, the generator injects interactive stations, adds walls to match the desired obstacle density, places agents, and finally prunes unreachable tiles.

comparison across difficulty levels. Level 1 tasks are designed such that existing methods can achieve reasonably high scores, enabling better comparisons and behavioral analysis. Higher levels are intended to challenge future methods. Although we currently include three difficulty levels, it is straightforward to extend the framework. While obstacle density has a practical upper bound, grid size can be increased arbitrarily to scale up environment complexity.

4.4 Task Sequences

Rather than a continuous domain shift, MEAL sequences involve discrete task boundaries, where agents transition between clearly distinct environments. By default, the task ID is accessible, aligning with the task-incremental learning paradigm.

4.5 Evaluation Metrics

We evaluate methods on three core metrics: **Average Performance**, **Forgetting**, and **Plasticity**. Let $s_i(j)$ denote the normalized score (see Section 4.1) on task j after training on task i , and let the task sequence consist of N tasks.

Average Performance We define average performance as the mean normalized score across all tasks at the end of training. This metric captures the balance between forward transfer and retention:

$$\mathcal{A} = \frac{1}{N} \sum_{i=1}^N s_N(i) \quad (1)$$

Forgetting Forgetting quantifies the degradation in performance on past tasks due to interference from training on later ones. For each task $i < N$, we compute the difference between the performance immediately after training and at the end of the sequence:

$$\mathcal{F} = \frac{1}{N-1} \sum_{i=1}^{N-1} (s_i(i) - s_N(i)) \quad (2)$$

Plasticity To evaluate continual training capacity over long task sequences, we measure the model’s ability to fit new tasks under continual learning constraints. We compute the average training score (i.e., final performance on the current task right after training) across the entire sequence:

$$\mathcal{P} = \frac{1}{N} \sum_{i=1}^N s_i(i) \quad (3)$$

This isolates how quickly and effectively the method learns a new task under capacity constraints, independently of retention. Unlike Average Performance, Plasticity does not require evaluation on previously seen tasks.

5 Experiments

5.1 Setup

The agent is trained on each task \mathcal{T}_i for $\Delta = 10^7$ environment steps on-policy with the dense reward setting, repeated over five seeds. During training, we evaluate the policy after every 100 updates by

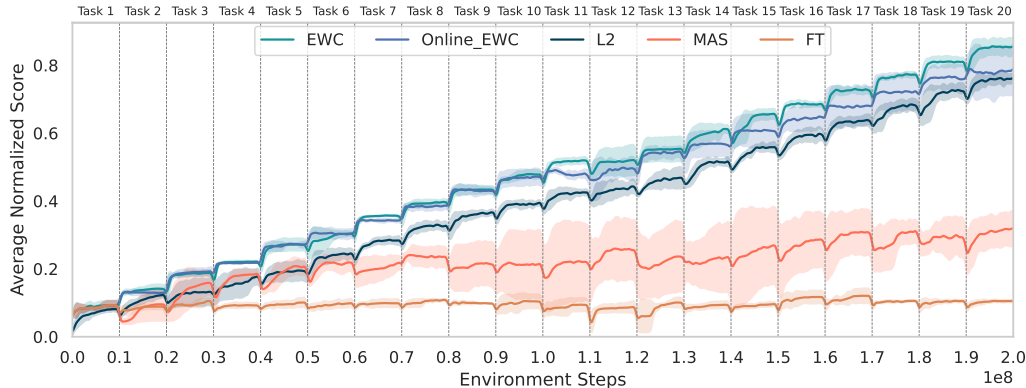


Figure 3: **Average Normalize Score** over the course of training on a sequence of 20 randomly generated Level 1 tasks. Shaded regions indicate 95% confidence intervals across 5 seeds.

running 10 evaluation episodes on all previously seen tasks. To enable fair comparisons across tasks with different layouts, sizes, and object configurations, we normalize raw returns by dividing the total number of soups delivered by a programmatically estimated upper bound specific to each layout (see Appendix A.1). This bound estimates the maximum number of soups a single agent could deliver in an episode by executing the most efficient cook-deliver cycle. A normalized score of 1 indicates the agent matches this single-agent optimum, while values above 1 indicate successful cooperation between agents that exceeds solo efficiency. We leverage JAX to reduce the wall-clock time for training on a single environment to around 5 minutes. All experiments are conducted on a dedicated compute node with a 72-core 3.2 GHz AMD EPYC 7F72 CPU and a single NVIDIA A100 GPU. We adopt many of JaxMARL’s default settings for our network configuration, IPPO setup, and training processes. For exact hyperparameters please refer to Appendix B.2.

5.2 Baselines

We evaluate several continual learning methods. Fine-Tuning (**FT**) is a naive baseline where the policy is trained sequentially across tasks without any mechanism to prevent forgetting. **L2-Regularization** [16] adds a penalty on parameter changes to encourage stability. **EWC** [16] is a regularization method that penalizes changes to important parameters, with importance measured using the Fisher Information Matrix. **Online EWC** is a variant that maintains a running estimate of parameter importance, making it more suitable for longer sequences. **MAS** [3] computes importance based on how parameters influence the policy’s output, rather than gradients. As the MARL baseline, we opt for **IPPO** [9]. It is a natural choice as it can be seamlessly integrated with all continual learning methods. It has been shown to outperform other MARL approaches on both SMAC [9] and Overcooked [25], making it a strong candidate for evaluating CMARL in a fully observable setting.

5.3 Baseline Comparison

Figure 3 compares the performance of several continual learning methods combined with IPPO over a 20-task sequence, and Table 2 reports summary metrics over 5 seeds. Fine-Tuning (FT) shows the highest plasticity, but fails catastrophically at retention: once a task is left behind, its performance rapidly collapses. EWC and L2 retain knowledge nearly perfectly, with EWC also achieving the highest average performance. Online EWC matches their plasticity but retains less. MAS ends up in the middle: moderate forgetting and low

Table 2: \mathcal{A} denotes final average performance, \mathcal{F} quantifies forgetting, and \mathcal{P} reflects plasticity. EWC and L2 retain knowledge best, with EWC achieving the highest overall performance. FT shows the highest plasticity but forgets almost everything.

Method	$\mathcal{A} \uparrow$	$\mathcal{F} \downarrow$	$\mathcal{P} \uparrow$
FT	0.048 \pm 0.00	0.899 \pm 0.01	1.163 \pm 0.03
Online EWC	0.769 \pm 0.09	0.150 \pm 0.09	1.136 \pm 0.03
EWC	0.839 \pm 0.03	0.031 \pm 0.03	1.062 \pm 0.01
MAS	0.281 \pm 0.07	0.501 \pm 0.06	0.914 \pm 0.07
L2	0.753 \pm 0.02	0.031 \pm 0.00	0.869 \pm 0.08

plasticity, resulting in significantly lower final performance.

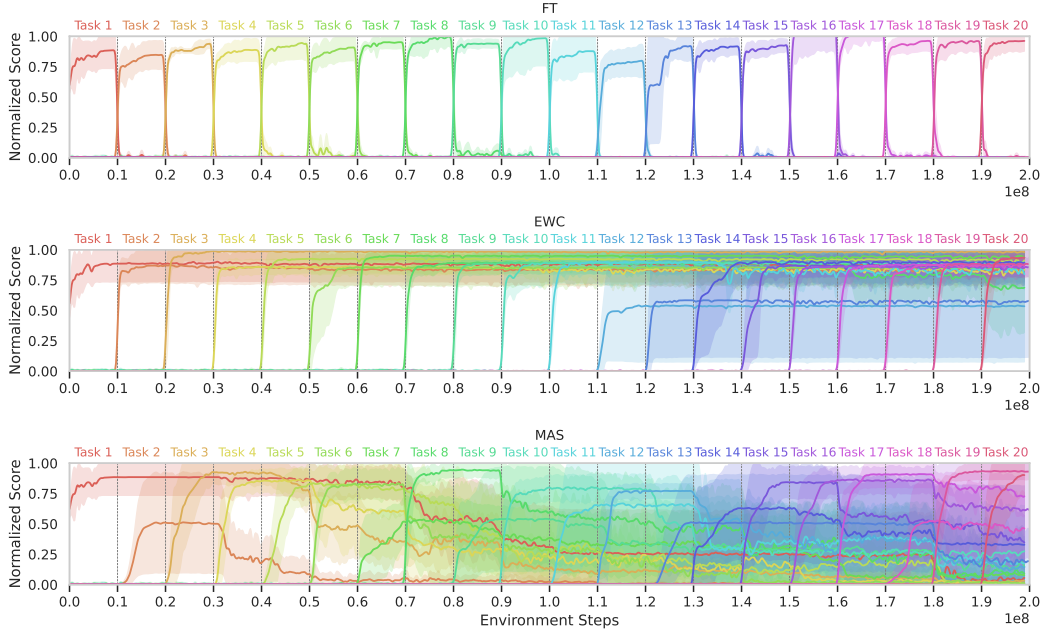


Figure 4: Normalized evaluation scores of each task in a Level 1 20-task sequence during training. Results are averaged over 5 seeds with the shaded areas depicting 95% confidence intervals.

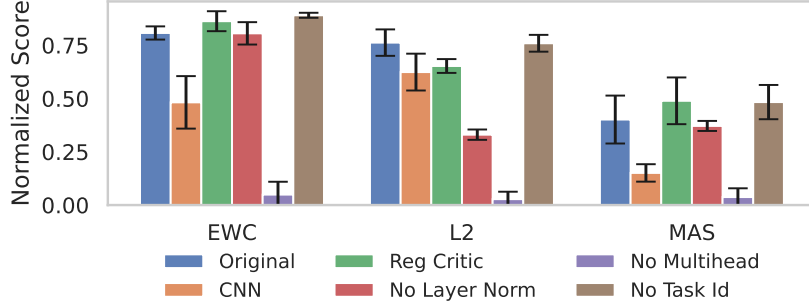


Figure 5: Ablation results for EWC, MAS, and L2 on Level 1 10-task sequences. The error bars indicate the 95% confidence interval across 5 seeds. Removing the multi-head architecture leads to severe performance degradation across all methods. Including the task ID and critic regularization have a negligible effect. Layer normalization has little impact on EWC or MAS, but significantly improves L2. A CNN encoder yields worse results than an MLP variant.

5.4 Forgetting

Figure 4 illustrates the extent of forgetting across tasks for Fine-Tuning (FT), EWC, and MAS. FT suffers from clear catastrophic forgetting: once the agent transitions to a new task, performance on the previous task collapses immediately. In contrast, EWC shows near-perfect retention across the sequence, maintaining stable performance on all tasks. MAS falls in between: it neither retains past knowledge effectively nor reaches the same per-task performance as FT or EWC, suggesting it struggles with both plasticity and stability in this setting.

5.5 Ablation Study

To determine which components are crucial for CMARL on MEAL, we ablate five components in our default IPPO learning setup: multi-head architectures, task identity inputs, critic regularization, layer normalization, and replacing the MLP with a CNN encoder. The results in Figure 5 reveal that multi-head outputs are most critical for MEAL task sequences. Removing them consistently

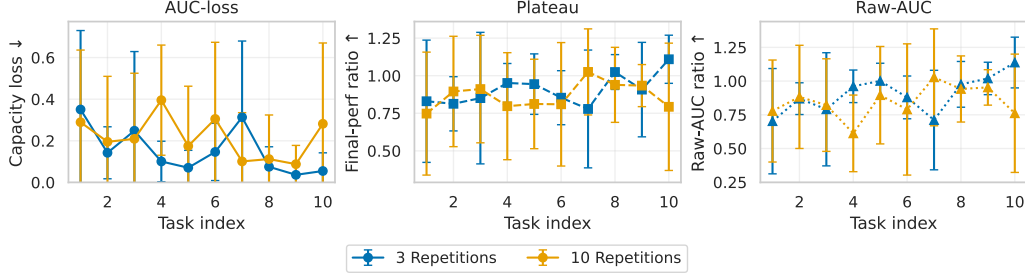


Figure 6: **Plasticity degradation in MEAL under fine-tuning (FT)**. We measure capacity loss (left), final-performance ratio (middle), and raw-AUC ratio (right) over a sequence of 10 tasks. Each line shows the mean across 5 seeds; error bars denote ± 1 s.e. Increasing the repetition count from 3 to 10 amplifies degradation across all metrics, indicating reduced plasticity as learning progresses.

devastates performance across all methods, likely due to uncontrolled interference between tasks in the shared output head. In contrast, not providing the model with the one-hot encoded task ID vector has a negligible effect. Prior continual RL studies [31, 30] report that it is beneficial to only regularize the actor and let the critic adapt freely. In our experiments, however, we find that this has little effect. Layer normalization shows method-specific sensitivity: while it makes little difference for EWC and MAS, it more than doubles the performance of L2 regularization. This is likely because L2 penalizes absolute weight magnitudes, and layer norm helps stabilize activations across tasks, mitigating harmful scale drift. Finally, swapping to a CNN encoder substantially hurts performance for all methods. Given the small layouts in Level 1 tasks (6×6 to 7×7), CNNs struggle to extract meaningful features and add unnecessary parameter overhead, making simple MLPs the better fit in this setting.

5.6 Network Plasticity

A well-documented pitfall in continual RL is the gradual loss of **plasticity**, an agent’s ability to fit new data after many tasks [1, 10]. To test whether MEAL exhibits the same pathology, we repeat a Level 1 10-task sequence multiple times and compare performance between repetitions. We evaluate the fine-tuning (FT) baseline, as it ranks highest in plasticity according to Table 2.

We track three standard metrics, each normalized to the initial repetition: (i) **AUC-loss** \downarrow captures capacity drop, (ii) Final-performance ratio (**FPR**) \uparrow compares the final plateau to the first repetition, and (iii) Raw-AUC ratio (**RAUC**) \uparrow measures total reward accumulated during the repeat. For formal definitions of the metrics and training curves, see Appendix C.2. Figure 6 shows that repeating tasks 10 times leads to a consistently greater loss of plasticity across all metrics, compared to 3 repetitions, in most tasks. Table 3 summarises the sequence-level means: AUC-loss rises $\approx 40\%$, while FPR drops below 1, and RAUC falls 6.5%, confirming that MEAL triggers the same degradation seen in single-agent continual RL.

Table 3: Averaged plasticity metrics for FT.

Repeats	AUC-loss \downarrow	FPR \uparrow	RAUC \uparrow
3	0.154	1.228	0.905
10	0.215	0.896	0.846

6 Conclusion

We introduced MEAL, the first benchmark for continual multi-agent reinforcement learning. By leveraging JAX for efficient GPU-accelerated training and introducing a diverse set of handcrafted and procedurally generated Overcooked environments, MEAL enables the study of long-horizon continual learning in cooperative settings. Our evaluation of six continual learning methods combined with the IPPO algorithm reveals that existing CL techniques struggle to retain cooperative behaviors while maintaining adaptability to new tasks. Regularization-based methods mitigate forgetting but sacrifice plasticity, while parameter-isolation methods fail to scale with longer task sequences. These findings highlight the need for new approaches that can handle the dual challenges of cooperation and non-stationarity in CMARL. We hope MEAL serves as a foundation for advancing this underexplored but important research direction.

7 Limitations

While MEAL provides a scalable and diverse testbed for continual multi-agent reinforcement learning, several limitations remain. First, MEAL is restricted to fully observable, two-agent environments with discrete action spaces, limiting its applicability to partially observable or competitive multi-agent settings. Second, while layout diversity is high, the domain itself is narrow. Overcooked dynamics do not capture the full complexity of real-world multi-agent interactions involving language, negotiation, or long-horizon planning. Third, our benchmark only evaluates task-incremental learning by changing layouts. Future work could extend MEAL to other continual learning settings. Finally, we only consider continual learning in settings where the environment layout changes across tasks, but not the partner agent or environment dynamics.

References

- [1] Zaheer Abbas, Rosie Zhao, Joseph Modayil, Adam White, and Marlos C Machado. Loss of plasticity in continual deep reinforcement learning. In *Conference on lifelong learning agents*, pages 620–636. PMLR, 2023.
- [2] John P Agapiou, Alexander Sasha Vezhnevets, Edgar A Duéñez-Guzmán, Jayd Matyas, Yiran Mao, Peter Sunehag, Raphael Köster, Udari Madhushani, Kavya Kopparapu, Ramona Comanescu, et al. Melting pot 2.0. *arXiv preprint arXiv:2211.13746*, 2022.
- [3] Rahaf Aljundi, Francesca Babiloni, Mohamed Elhoseiny, Marcus Rohrbach, and Tinne Tuytelaars. Memory aware synapses: Learning what (not) to forget. In *Proceedings of the European conference on computer vision (ECCV)*, pages 139–154, 2018.
- [4] Craig Atkinson, Brendan McCane, Lech Szymanski, and Anthony Robins. Pseudo-rehearsal: Achieving deep reinforcement learning without catastrophic forgetting. *Neurocomputing*, 428: 291–307, 2021.
- [5] James Bradbury, Roy Frostig, Peter Hawkins, Matthew James Johnson, Chris Leary, Dougal Maclaurin, George Necula, Adam Paszke, Jake VanderPlas, Skye Wanderman-Milne, and Qiao Zhang. JAX: composable transformations of Python+NumPy programs, 2018. URL <http://github.com/jax-ml/jax>.
- [6] Micah Carroll, Rohin Shah, Mark K. Ho, Thomas Griffiths, Sanjit Seshia, Pieter Abbeel, and Anca Dragan. On the utility of learning about humans for human-ai coordination. In *Advances in Neural Information Processing Systems (NeurIPS)*, volume 32, 2019. URL https://proceedings.neurips.cc/paper_files/paper/2019/file/f5b1b89d3db40d65b49f8f9e383ac5dd-Paper.pdf.
- [7] Feng Chen, Fuguang Han, Cong Guan, Lei Yuan, Zhilong Zhang, Yang Yu, and Zongzhang Zhang. Stable continual reinforcement learning via diffusion-based trajectory replay. *arXiv preprint arXiv:2411.10809*, 2024.
- [8] Wesley Chung, Lynn Cherif, Doina Precup, and David Meger. Parseval regularization for continual reinforcement learning. *Advances in Neural Information Processing Systems*, 37: 127937–127967, 2024.
- [9] Christian Schroeder De Witt, Tarun Gupta, Denys Makoviichuk, Viktor Makovychuk, Philip HS Torr, Mingfei Sun, and Shimon Whiteson. Is independent learning all you need in the starcraft multi-agent challenge? *arXiv preprint arXiv:2011.09533*, 2020.
- [10] Shibhansh Dohare, J Fernando Hernandez-Garcia, Qingfeng Lan, Parash Rahman, A Rupam Mahmood, and Richard S Sutton. Loss of plasticity in deep continual learning. *Nature*, 632 (8026):768–774, 2024.
- [11] Zeki Doruk Erden, Donia Gasmi, and Boi Faltings. Continual reinforcement learning via autoencoder-driven task and new environment recognition. In *The Seventeenth Workshop on Adaptive and Learning Agents*.

- [12] Jakob Foerster, Gregory Farquhar, Triantafyllos Afouras, Nantas Nardelli, and Shimon Whiteson. Counterfactual multi-agent policy gradients. In *Proceedings of the AAAI conference on artificial intelligence*, volume 32, 2018.
- [13] Muhammad Burhan Hafez and Kerim Erekmén. Continual deep reinforcement learning with task-agnostic policy distillation. *Scientific Reports*, 14(1):31661, 2024.
- [14] Pablo Hernandez-Leal, Bilal Kartal, and Matthew E Taylor. A survey and critique of multiagent deep reinforcement learning. *Autonomous Agents and Multi-Agent Systems*, 33(6):750–797, 2019.
- [15] Hengyuan Hu, Adam Lerer, Alex Peysakhovich, and Jakob Foerster. “other-play” for zero-shot coordination. In *International Conference on Machine Learning*, pages 4399–4410. PMLR, 2020.
- [16] James Kirkpatrick, Razvan Pascanu, Neil Rabinowitz, Joel Veness, Guillaume Desjardins, Andrei A Rusu, Kieran Milan, John Quan, Tiago Ramalho, Agnieszka Grabska-Barwinska, et al. Overcoming catastrophic forgetting in neural networks. *Proceedings of the national academy of sciences*, 114(13):3521–3526, 2017.
- [17] Paul Knott, Micah Carroll, Sam Devlin, Kamil Ciosek, Katja Hofmann, Anca D Dragan, and Rohin Shah. Evaluating the robustness of collaborative agents. *arXiv preprint arXiv:2101.05507*, 2021.
- [18] Karol Kurach, Anton Raichuk, Piotr Stańczyk, Michał Zajac, Olivier Bachem, Lasse Espeholt, Carlos Riquelme, Damien Vincent, Marcin Michalski, Olivier Bousquet, et al. Google research football: A novel reinforcement learning environment. In *Proceedings of the AAAI conference on artificial intelligence*, volume 34, pages 4501–4510, 2020.
- [19] Ryan Lowe, Yi I Wu, Aviv Tamar, Jean Harb, OpenAI Pieter Abbeel, and Igor Mordatch. Multi-agent actor-critic for mixed cooperative-competitive environments. *Advances in neural information processing systems*, 30, 2017.
- [20] Arun Mallya and Svetlana Lazebnik. Packnet: Adding multiple tasks to a single network by iterative pruning. In *Proceedings of the IEEE conference on Computer Vision and Pattern Recognition*, pages 7765–7773, 2018.
- [21] Igor Mordatch and Pieter Abbeel. Emergence of grounded compositional language in multi-agent populations. In *Proceedings of the AAAI conference on artificial intelligence*, volume 32, 2018.
- [22] Afshin OroojlooyJadid and Davood Hajinezhad. A review of cooperative multi-agent deep reinforcement learning. *arXiv preprint arXiv:1908.03963*, 2019.
- [23] Sam Powers, Eliot Xing, Eric Kolve, Roozbeh Mottaghi, and Abhinav Gupta. Cora: Benchmarks, baselines, and metrics as a platform for continual reinforcement learning agents. In *Conference on Lifelong Learning Agents*, pages 705–743. PMLR, 2022.
- [24] Tabish Rashid, Mikayel Samvelyan, Christian Schroeder De Witt, Gregory Farquhar, Jakob Foerster, and Shimon Whiteson. Monotonic value function factorisation for deep multi-agent reinforcement learning. *Journal of Machine Learning Research*, 21(178):1–51, 2020.
- [25] Alexander Rutherford, Benjamin Ellis, Matteo Gallici, Jonathan Cook, Andrei Lupu, Garðar Ingvarsson, Timon Willi, Akbir Khan, Christian Schroeder de Witt, Alexandra Souly, et al. Jaxmarl: Multi-agent rl environments and algorithms in jax. In *Proceedings of the 23rd International Conference on Autonomous Agents and Multiagent Systems*, pages 2444–2446, 2024.
- [26] Mikayel Samvelyan, Tabish Rashid, Christian Schroeder De Witt, Gregory Farquhar, Nantas Nardelli, Tim GJ Rudner, Chia-Man Hung, Philip HS Torr, Jakob Foerster, and Shimon Whiteson. The starcraft multi-agent challenge. *arXiv preprint arXiv:1902.04043*, 2019.
- [27] Artyom Y Sorokin and Mikhail S Burtsev. Continual and multi-task reinforcement learning with shared episodic memory. *arXiv preprint arXiv:1905.02662*, 2019.

- [28] DJ Strouse, Kevin McKee, Matt Botvinick, Edward Hughes, and Richard Everett. Collaborating with humans without human data. *Advances in Neural Information Processing Systems*, 34: 14502–14515, 2021.
- [29] Peter Sunehag, Guy Lever, Audrunas Gruslys, Wojciech Marian Czarnecki, Vinicius Zambaldi, Max Jaderberg, Marc Lanctot, Nicolas Sonnerat, Joel Z Leibo, Karl Tuyls, et al. Value-decomposition networks for cooperative multi-agent learning. *arXiv preprint arXiv:1706.05296*, 2017.
- [30] Tristan Tomilin, Meng Fang, Yudi Zhang, and Mykola Pechenizkiy. Coom: a game benchmark for continual reinforcement learning. *Advances in Neural Information Processing Systems*, 36, 2023.
- [31] Maciej Wołczyk, Michał Zając, Razvan Pascanu, Łukasz Kuciński, and Piotr Miłoś. Continual world: A robotic benchmark for continual reinforcement learning. *Advances in Neural Information Processing Systems*, 34:28496–28510, 2021.
- [32] Sarah A Wu, Rose E Wang, James A Evans, Joshua B Tenenbaum, David C Parkes, and Max Kleiman-Weiner. Too many cooks: Bayesian inference for coordinating multi-agent collaboration. *Topics in Cognitive Science*, 13(2):414–432, 2021.
- [33] Chao Yu, Akash Velu, Eugene Vinitsky, Jiaxuan Gao, Yu Wang, Alexandre Bayen, and Yi Wu. The surprising effectiveness of ppo in cooperative multi-agent games. *Advances in neural information processing systems*, 35:24611–24624, 2022.
- [34] Lei Yuan, Ziqian Zhang, Lihe Li, Cong Guan, and Yang Yu. A survey of progress on cooperative multi-agent reinforcement learning in open environment. *arXiv preprint arXiv:2312.01058*, 2023.
- [35] Lei Yuan, Lihe Li, Ziqian Zhang, Fuxiang Zhang, Cong Guan, and Yang Yu. Multiagent continual coordination via progressive task contextualization. *IEEE Transactions on Neural Networks and Learning Systems*, 2024.
- [36] Friedemann Zenke, Ben Poole, and Surya Ganguli. Continual learning through synaptic intelligence. In *International conference on machine learning*, pages 3987–3995. PMLR, 2017.

A Implementation Details

A.1 Maximum Soup Delivery Estimator

Let a kitchen layout \mathcal{L} be defined by four disjoint sets of tiles (onion piles \mathcal{O} , plate piles \mathcal{P} , pots \mathcal{K} , delivery counters \mathcal{G}) and a set of walls \mathcal{W} . A tile (x, y) is *walkable* if $(x, y) \notin \mathcal{W}$.

Neighbourhood of an object family. We denote the set of walkable tiles adjacent (in the 4-neighbour sense) to any object in \mathcal{S} as:

$$\mathcal{N}(\mathcal{S}) = \{(x', y') \mid (x, y) \in \mathcal{S}, \|(x', y') - (x, y)\|_1 = 1, (x', y') \notin \mathcal{W}\}$$

Shortest obstacle-aware distance. Given two tile sets $A, B \subseteq \mathbb{Z}^2$, we define

$$d(A, B) = \min_{a \in A, b \in B} \text{dist}_{\text{manhattan}}^{\mathcal{G}_{\mathcal{L}}}(a, b),$$

where $\mathcal{G}_{\mathcal{L}}$ is the grid graph induced by walkable tiles. We realize this via a breadth-first search (BFS).

Single-agent cook-deliver cycle. A soup requires three onions, one plate pick-up, one soup pick-up, and one delivery. Let

$$d_{\text{onion}} = d(\mathcal{N}(\mathcal{O}), \mathcal{N}(\mathcal{K})), \quad d_{\text{plate}} = d(\mathcal{N}(\mathcal{P}), \mathcal{N}(\mathcal{K})), \quad d_{\text{goal}} = d(\mathcal{N}(\mathcal{K}), \mathcal{N}(\mathcal{G})).$$

The optimistic *movement cost* for one cycle is

$$c_{\text{move}} = 3 d_{\text{onion}} + d_{\text{plate}} + 1 + d_{\text{goal}} + 3.$$

Interaction overhead. Every pick-up or drop is assumed to take a constant $c_{\text{act}} = 2$ steps (turn + interact). With $n_{\text{int}} = 3 \times 2 + 1 + 1 + 1 = 9$ interactions per cycle, the overhead is $c_{\text{cover}} = n_{\text{int}} c_{\text{act}} = 18$.

Cycle time and upper bound. Including the fixed cooking time $c_{\text{cook}} = 20$ steps, the single-agent cycle time is

$$T_{\text{cycle}} = c_{\text{move}} + c_{\text{cook}} + c_{\text{cover}}.$$

For an episode horizon H , we upper-bound the number of soups by

$$N_{\text{max}}(\mathcal{L}, H) = \lfloor H / T_{\text{cycle}} \rfloor,$$

and convert it to reward with $r_{\text{deliver}} = 20$:

$$R_{\text{max}}(\mathcal{L}, H) = 20 N_{\text{max}}(\mathcal{L}, H).$$

The bound assumes *a single agent acting optimally*. It ignores multi-agent collaboration and therefore *underestimates* throughput in layouts where multiple agents can parallelize the workflow. Listing 1 contains the exact implementation.

A.2 Procedural Kitchen Generator

Objective. Given a random seed and user-selectable parameters (number of agents n_a , layout height range $[h_{\min}, h_{\max}]$, layout width range $[w_{\min}, w_{\max}]$, and wall-density ρ), the goal is to emit a *solvable* grid string G representing the Overcooked environment.

A.2.1 Notation

Let $h, w \sim \text{UniformInt}(h_{\min}, h_{\max}), \text{UniformInt}(w_{\min}, w_{\max})$, and denote by $\mathcal{C} = \{(i, j) \mid 1 \leq i \leq h - 2, 1 \leq j \leq w - 2\}$ the set of *internal* cells (outer walls excluded). Its cardinality is $N_{\text{int}} = (h - 2)(w - 2)$. An *unpassable* cell contains either a hard wall (#) or an interactive tile; we write $N_{\text{unpass}}(G)$ for the number of such cells in G .

Listing 1 Heuristic upper bound (estimate_max_soup).

```
# overcooked_upper_bound.py      (excerpt)
DELIVERY_REWARD = 20
COOK_TIME = 20
ACTION_OVERHEAD = 2
INTERACTIONS_PER_CYCLE = 3 * 2 + 1 + 1 + 1
OVERHEAD_PER_CYCLE = INTERACTIONS_PER_CYCLE * ACTION_OVERHEAD

def estimate_cycle_time(layout, n_agents=2):
    ...
    move_cost = 3 * d_onion + d_plate + 1 + d_goal + 3
    return move_cost + COOK_TIME + OVERHEAD_PER_CYCLE

def estimate_max_soup(layout, episode_len, n_agents=2):
    cyc = estimate_cycle_time(layout, n_agents)
    soups = episode_len // cyc
    return int(soups * DELIVERY_REWARD)
```

A.2.2 Algorithm

The generator performs the following loop until a valid grid is produced (Listing 2):

1. **Draw size.** Sample h, w and create an $h \times w$ matrix initialised to FLOOR tiles, then overwrite the border with WALL.
2. **Place interactive tiles.** For each symbol in {GOAL, POT, ONION_PILE, PLATE_PILE} choose a random multiplicity $m \in \{1, 2\}$ and stamp the symbol onto m uniformly chosen floor cells.
3. **Inject extra walls.** Let $n_{\text{target}} = \lceil \rho N_{\text{int}} \rceil$ and $n_{\text{add}} = \max(0, n_{\text{target}} - N_{\text{unpass}}(G))$. Place n_{add} additional walls on random floor cells.
4. **Place agents.** Stamp n_a AGENT symbols on random remaining floor cells.
5. **Validate.** Run the deterministic evaluate_grid solver; if it returns True, terminate and return (G) , otherwise restart.
6. **Cleanup.** Remove any interactive elements and tiles that are unreachable from all agent positions.
7. **Return.** Output the final grid.

Solvability criterion. The validator (Appendix A.3) checks (i) path connectivity between every agent and each interactive tile family, (ii) at least one pot reachable from an onion pile and a plate pile, and (iii) at least one goal reachable from a pot. This is implemented via multiple breadth-first searches. Appendix A.3 further details the evaluator logic.

Wall-density effect. Because interactive tiles themselves count as obstacles, the algorithm first places them, then *only as many extra walls as needed* to reach the prescribed obstacle ratio ρ . This keeps difficulty roughly constant even when two copies of every station are spawned.

Failure handling. If any placement stage exhausts the pool of empty cells, or the validator rejects the grid, the attempt is aborted and restarted with a fresh h, w sample. We cap retries at `max_attempts` (default 2000); empirically fewer than five attempts suffice for $\rho \leq 0.3$.

Complexity. All placement operations are $O(hw)$ in the worst case (linear scans to collect empty cells), while validation runs a constant number of BFS passes, each $O(hw)$. Hence one successful attempt is $O(hw)$.

Listing 2 Overcooked Layout Generator

```
def generate_random_layout(seed, params):
    rng = random.Random(seed)
    for attempt in range(params.max_attempts):
        h = rng.randint(*params.h_range)
        w = rng.randint(*params.w_range)
        grid = init_floor_with_border(h, w)

        # 1. Interactive tiles
        for sym in [GOAL, POT, ONION_PILE, PLATE_PILE]:
            if not place_random(grid, sym, rng.randint(1, 2), rng):
                break # restart

        # 2. Extra walls to hit density
        n_target = round(params.wall_density * (h-2)*(w-2))
        n_add = n_target - count_unpassable(grid)
        if not place_random(grid, WALL, n_add, rng):
            continue # restart

        # 3. Agents
        if not place_random(grid, AGENT, params.n_agents, rng):
            continue

        # 4. Validate
        if evaluate_grid(to_string(grid)):
            return to_string(grid)
```

A.3 Layout Validator

We guarantee that every procedurally generated kitchen is *playable* by running a deterministic validator before training begins. The validator implements ten checks, ranging from basic grid sanity to cooperative reachability. A grid is accepted only if **all** checks pass.

Notation. Let G be an $h \times w$ character matrix with symbols $\{W, X, O, B, P, A, \}$ for walls, delivery, onion pile, plate pile, pot, agent, and floor. Interactive tiles are $\mathcal{I} = \{X, O, B, P\}$, and unpassable tiles $\mathcal{U} = \mathcal{I} \cup \{W\}$.

Validation rules.

- R1** *Rectangularity* – all rows have equal length.
- R2** *Required symbols* – each of W, X, O, B, P, A appears at least once.
- R3** *Border integrity* – every outer-row/column tile is in $\{W\} \cup \mathcal{I}$.
- R4** *Interactivity access* – every tile in $\mathcal{I} \cup \{A\}$ has at least one 4-neighbour that is A or floor.
- R5** *Reachable onions* – at least one onion pile is reachable by some agent.
- R6** *Usable pots* – at least one pot is reachable *and* lies in the same connected component as a reachable onion.
- R7** *Usable delivery* – at least one delivery tile is reachable *and* lies in a component with a usable pot.
- R8** *Agent usefulness* – each agent can either interact with an object directly or participate in a hand-off (adjacent wall shared with the other agent’s region).
- R9** *Coverage* – the union of agents’ reachable regions touches every object family in \mathcal{I} .
- R10** *Handoff counter* – if one agent cannot reach all families, a wall tile adjacent to *both* regions exists, enabling item transfer.

Rules R5–R10 rely on two depth-first searches (DFS) from the agent positions. The DFS explores floor and agent tiles only; whenever it touches an interactive tile, that family is marked as “found.” Let $\text{Reach}_k \subseteq [h] \times [w]$ denote tiles reached from agent k ($k \in \{1, 2\}$).

Algorithmic outline. Listing 3 shows a condensed version of the validator.

Listing 3 Condensed Layout Validator.

```
def validate(grid_str):
    g = [list(r) for r in grid_str.splitlines()]
    h, w = len(g), len(g[0])

    # R1-R3 omitted for brevity ...

    # Depth-first search from a start cell
    def dfs(i, j, seen):
        if (i, j) in seen or g[i][j] in UNPASSABLE_TILES - {AGENT}:
            return
        seen.add((i, j))
        for di, dj in ((1,0),(-1,0),(0,1),(0,-1)):
            dfs(i+di, j+dj, seen)

    # Agents and family reachability
    a1, a2 = [(i, j) for i,r in enumerate(g)
               for j,c in enumerate(r) if c == AGENT]
    reach1, reach2 = set(), set()
    dfs(*a1, reach1); dfs(*a2, reach2)

    # Helper: reachable( $\mathcal{S}$ , reach)
    def any_reach(symbols, reach):
        return any(g[i][j] in symbols for i,j in reach)

    # R5-R7
    if not any_reach({ONION_PILE}, reach1|reach2):
        return False
    if not any_reach({POT}, reach1|reach2):
        return False
    if not any_reach({GOAL}, reach1|reach2):
        return False

    # R8-R10 (usefulness & hand-off)
    def useful(reach_me, reach_other):
        # direct or shared-wall hand-off
        for i,j in reach_me:
            if g[i][j] in INTERACTIVE_TILES: return True
            if g[i][j] == FLOOR and any(
                (abs(i-i2)+abs(j-j2)) == 1 and g[i2][j2] == WALL)
                for i2,j2 in reach_other):
                return True
        return False

    if not useful(reach1, reach2): return False
    if not useful(reach2, reach1): return False
    return True
```

Complexity. All checks are $O(hw)$ and require only two DFS traversals, thus one validation runs in time linear to the grid area and is negligible compared with policy learning.

Practical impact. In practice, fewer than 1% of generator attempts fail validation when wall-density $\rho \leq 0.15$ and kitchen size $\geq 8 \times 8$. We therefore cap retries at 2000 without noticeable overhead.

B Experimental Setup

B.1 Network Architecture

All agents share the same actor–critic backbone, implemented in Flax. Two encoder variants are provided:

- **MLP** (default): observation tensor is flattened to a vector and passed through $\{2, 3\}$ fully-connected layers of width 128.
- **CNN**: three 32-channel convolutions with kernel sizes 5×5 , 3×3 , 3×3 feed a 64-unit projection, followed by a single 128-unit dense layer.

Common design knobs (controlled from the CLI) are:

- **Activation** (`relu` vs. `tanh`).
- **LayerNorm**: applied after every hidden layer when `use_layer_norm` is enabled.
- **Shared vs. Separate encoder**: with `shared_backbone` the two heads operate on a common representation; otherwise actor and critic keep independent trunks.
- **Multi-head outputs**: if `use_multihead` is set, each head holds a distinct slice of logits/values for every task (`num_tasks = |\mathcal{T}|`). The correct slice is selected with the cheap tensor reshape in `choose_head`.
- **Task-one-hot conditioning**: setting `use_task_id` concatenates a one-hot vector of length $|\mathcal{T}|$ before the actor/critic heads, mimicking “oracle” task identifiers used in many CL papers.

All linear/conv layers use orthogonal weight initialisation with gain $\sqrt{2}$ (or 0.01 for policy logits) and zero biases. The policy outputs a `distrax.Categorical`; the critic outputs a scalar.

B.2 Hyperparameters

Table 4 lists settings that are *constant* across every experiment unless stated otherwise. Values match the `Config` dataclass in the training script.

Table 4: Fixed hyper-parameters. All experiments use dense reward shaping, two agents, and IPPO unless noted. CL coefficients λ refer to the regularisation strength passed to each method.

Parameter	Value
<i>Optimisation (IPPO)</i>	
Learning rate η	3×10^{-4}
LR annealing	linear ($3 \times 10^{-4} \rightarrow 0$)
Env. steps per task Δ	10^7
Parallel envs	16
Rollout length T	128
Update epochs	8
Minibatches / update	8
Effective batch size	$16 \times 128 = 2048$
Discount γ	0.99
GAE λ	0.957
PPO clip ϵ	0.2
Entropy coef. α_{ent}	0.01
Value-loss coef. α_{vf}	0.5
Max grad-norm	0.5
<i>Continual-learning specifics</i>	
Sequence length $ \mathcal{T} $	20 (base sequence), repeated r times
Reg. coefficient λ	10^{11} (EWC), 10^9 (MAS), 10^7 (L2)
EWC decay	0.9
Importance episodes / steps	5 / 500
Regularise critic / heads	No / No
<i>Miscellaneous</i>	
Reward shaping horizon	2.5×10^6 steps (linear to 0)
Evaluation interval	every 100 updates (10 episodes)
Random seeds	$\{1 \dots 5\}$

C Extended Results

In this section, we provide additional details, results, and analysis of our experiments.

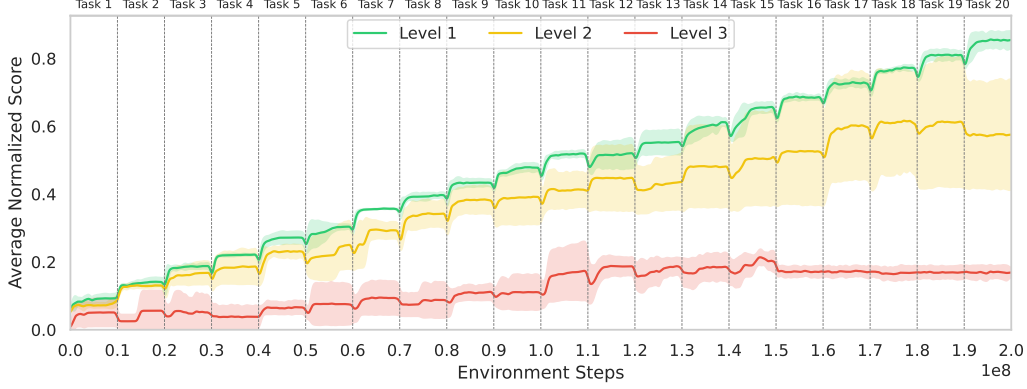


Figure 7: **Average Normalized Score** over the course of training EWC on a sequence of 20 randomly generated tasks per difficulty level. Shaded regions indicate 95% confidence intervals across 5 seeds.

C.1 Difficulty Levels

Higher difficulty levels pose greater challenges for both learning and retention. As the grid size and obstacle density increase, the environment becomes more complex: interactable items are farther apart, and navigation paths are longer and more convoluted. This increases the number of steps required to complete a recipe, making the overall task harder to memorize and reproduce. Higher-level layouts also add demands for plasticity and transfer. The larger layout space introduces greater variability between tasks, making it harder to reuse learned behavior. These factors collectively lead to lower performance as difficulty increases, as shown in Figure 7.

C.2 Network Plasticity

C.2.1 Metrics

We follow Abbas et al. [1], Dohare et al. [10] and quantify **plasticity**, the ability to fit fresh data after many tasks, by three complementary metrics computed from the training reward.

Notation. For a single task let r_t be the online reward at step $t \leq T$. A repetition experiment presents the same task R times, so the trace splits into R contiguous segments of equal length $L = T/R$. We smooth r_t with a Gaussian kernel (bandwidth σ) and define the cumulative average

$$\bar{r}(t) = \frac{1}{t} \sum_{i=1}^t r_i, \quad t = 1, \dots, L.$$

All metrics compare a later repetition $j > 0$ with the *baseline* repetition $j = 0$.

AUC-loss. Let $\text{AUC}_j = \int_0^L \bar{r}_j(t) dt$. The capacity drop for repetition j is

$$\text{loss}_j = 1 - \frac{\text{AUC}_j}{\text{AUC}_0}, \quad j = 1, \dots, R-1, \quad (4)$$

where 0 indicates perfect retention. We report the mean of Eq. (4) over repetitions and seeds.

Final-Performance Ratio (FPR). With $p_j = \bar{r}_j(L-1)$ the plateau reward of repetition j ,

$$\text{FPR}_j = \frac{p_j}{p_0}, \quad j = 1, \dots, R-1, \quad (5)$$

so $\text{FPR}_j > 1$ implies no loss, $\text{FPR}_j < 1$ indicates degraded plateau performance.

Raw-AUC Ratio (RAUC). Using the *unsmoothed* running reward,

$$\text{RAUC}_j = \frac{\text{AUC}_j^{\text{raw}}}{\text{AUC}_0^{\text{raw}}}, \quad j = 1, \dots, R - 1, \quad (6)$$

which captures the total reward accumulated during learning. Higher values in Eq. (5)–Eq. (6) are better.

Sequence-level aggregation. For a task sequence of length $|\mathcal{T}|$ we compute the per-task means of (4)–(6) and average across tasks, yielding a single global score per repetition count R .

C.2.2 Training Curves

Figure 8 plots the mean normalized score of the fine-tuning (FT) baseline over ten repetitions. Performance on Tasks 8 and 9 remains virtually unchanged, indicating little to no plasticity loss. In contrast, Tasks 1, 2, 6, and 10 show a clear degradation: the agent fails to recover the score achieved during the first repetition, illustrating a pronounced loss of plasticity.

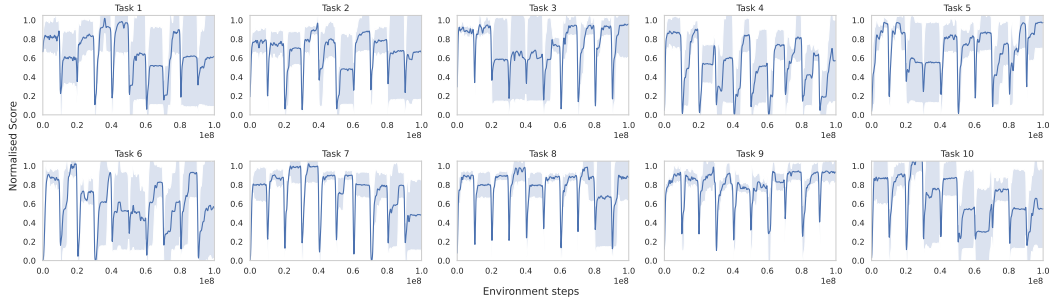


Figure 8: Training curves of FT across a Level 1 10-task sequence repeated ten times over 5 seeds.